Rod/Disk Coexistence in Dilute Soap Solutions

WILLIAM E. McMULLEN, AVINOAM BEN-SHAUL, AND WILLIAM M. GELBART[1]

Department of Chemistry and Biochemistry, University of California, Los Angeles 90024, California; Department of Physical Chemistry and the Fritz Haber Center for Molecular Dynamics, The Hebrew University, Jerusalem 91904, Israel; and Laboratoire de Physique des Solides, Université de Paris-Sud Orsay 91405, France

Received June 29, 1983; accepted October 5, 1983

Self-assembly theories for dilute micellar solutions generally assume that the chemical potential per surfactant is dominated by the "surface" terms $\gamma a + c/a$ where γa and c/a represent the interfacial and electrostatic energies associated with the head groups (having area a). That is, they suppress the energy and entropy of packing the hydrophobic chains (having volume v and length l). These "bulk" terms depend on the head group area *and also* on the elastic properties unique to the surfactant environments (e.g., thickness, curvature, etc.) in question: the chains are not "passive"—we cannot optimize the head group situation without taking into account the free energy "price" "paid" by the tails. In this paper we show that the differences in compressional and splay elasticities among the various environments (e.g., sphere, rod, disk, etc.) can be treated phenomenologically by defining a "relative stability" parameter y:

$$a_0 \frac{l}{v} \equiv 1 + y, \qquad 0 \leqslant y \leqslant 2 \qquad \left(a_0 = \sqrt{\frac{c}{\gamma}}\right).$$

For $y \geqslant 0$, only disks survive (as lamellae or finite micelles); for $y \simeq \sqrt{2} - 1$, rods and disks coexist with relative numbers and sizes determined by overall concentration; and for $y \leqslant 1$, the rods are dominant, with spheres taking over for still larger y. After relating y to physical properties of the surfactant and solvent conditions, we discuss our results in terms of recent theories of micellar shapes.

I. INTRODUCTION: THE ROLE OF "TAIL" ELASTICITY

Consider an isotropic solution of micelles over a concentration range for which the solution can be treated as ideal. In this case we can write

$$\tilde{\mu}_s = \tilde{\mu}_s^0 + \frac{kT}{s} \ln \frac{x_s}{s} \qquad [1]$$

for the chemical potential per surfactant in micelles consisting of s surfactants. Here $s\tilde{\mu}_s^0$ is the standard chemical potential associated with a *single* s-micelle at a specified point in the solution (1); $(kT/s) \ln X_s/s$ is the entropy of mixing associated with the *distribution* of different-sized micelles, each present with mole fraction x_s/s. Note that $x_s = N_s/N_T$, where N_s is the number of surfactant molecules incorporated into s-micelles and $N_T \equiv \sum_s N_s + N_w$ is the *total* number of molecules (surfactant, $\sum_s N_s$, plus water, N_w); accordingly, N_s/s isthe number of s-micelles, and x_s/s is their mole fraction, etc. Now, the system is in a state of chemical equilibrium with respect to the exchange of molecules between micelles. Denoting an s-aggregate by A_s we have then that all "reactions" of the form

$$sA_1 \rightleftharpoons A_s \qquad [2]$$

must be in equilibrium. (A_1 denotes the "monomer" or single, unaggregated surfactant molecule.) Consequently we must have $s\mu_1 = \mu_s \equiv s\tilde{\mu}_s$ for all s, or

[1] On sabbatical leave from September 1982 to June 1983. Permanent address: Department of Chemistry and Biochemistry, UCLA, Los Angeles 90024, California.

0021-9797/84 $3.00

$$\mu_1 = \tilde{\mu}_s \quad \text{for all } s \qquad [3]$$

Using [1] for μ_1 and $\tilde{\mu}_s$, it follows directly from [3] that

$$x_s = s x_1^s e^{\beta s(\mu_1^0 - \tilde{\mu}_s^0)}. \qquad [4]$$

Thus the equilibrium size distribution of micelles is determined by the s-dependence of $\tilde{\mu}_s^0$, as is already well appreciated (2, 3).

We shall be concerned in what follows with aggregate structures which consist each of two different surfactant environments. In rod-like micelles, for example, surfactants lie either in the prolate-cylindrical "body" or in the part-spherical "caps;" in "disks" they are found in the oblate-cylindrical "body" or in the part-toroidal "rim." The disk situation is more complicated because the "rim" must continuously adjust to the growth of the "body;" in rods, on the other hand, the "caps" can remain essentially constant as the "body" grows.

Let $\tilde{\mu}_i^0(a)$ denote the chemical potential of a surfactant in environment i, with head group area a. We write

$$\tilde{\mu}_i^0(a) = h_i(a) + g_i(a). \qquad [5]$$

Here $h_i(a)$ describes the usual (2, 3) interfacial tension and electrostatic energy contributions to the "surface" part of $\tilde{\mu}^0$. It is generally written phenomenologically as a sum $\gamma a + c/a$ where γa is the interfacial energy arising from the water/surfactant contact and c/a is the Coulomb repulsion between ionic heads; curvature corrections to $\gamma a + c/a$ are neglected. The $g_i(a)$ corresponds to the "bulk" energy and entropy effects associated with the packing of the hydrophobic tails. It is usually assumed to be constant ($\equiv g$), independent of i and a. But, in fact, it depends in a very complicated way—not just on the area per head group a, but also—on the nature (e.g., thickness and curvature) of the surfactant environment (i) in question. For example, the chemical potential of a chain (tail) in the part-spherical cap of a rod will be different from that of a chain *with the same head group area* in the prolate-cylindrical body. This is because the thickness and curvature are different in the two environments, implying an attendant difference in compressional and splay elasticity of the chains. In other words, the chains are not "passive"—we cannot optimize the head group situation without taking into account the free energy "price" "paid" by the tails.

Let $a_0^{(i)}$ denote the value of a which minimizes $\tilde{\mu}_i^0(a)$. If the a-dependent part of the "bulk" contributions $g_i(a)$ is negligible with respect to $\gamma a + c/a$, we will have $\{a_0^{(i)}\} \to a_0$, where a_0 is the a which optimizes the "surface" free energy $\gamma a + c/a$. Otherwise the head group area will not adjust to $a_0 = (c/\gamma)^{1/2}$ but rather to a value which depends on whether the surfactant in question lies, say, in a "cap" or "body" environment. Only by knowing the actual compressional and splay elasticity contributions to $g_i(a)$ can we determine the optimum head group areas which pertain to each environment. Nevertheless it is useful to proceed by simply recognizing that the $a_0^{(i)}$'s will in general be quite different from one another, thereby implying distinct $\tilde{\mu}_i^0(a_0^{(i)}) \equiv$ minimum $\tilde{\mu}_i^0$'s for each environment.

As is often discussed (3), the area per head group $a^{(i)}$ of a surfactant in a given environment i is uniquely related—via straightforward surface/volume geometric relations—to its thickness, l_i:

$$\frac{a^{(i)}}{v/l_i} = i = \begin{cases} 1, & \text{bilayer (lamellar)} \\ 2, & \text{cylinder (hexagonal)} \\ 3, & \text{sphere.} \end{cases} \qquad [6]$$

(This follows as soon as one assumes a uniform density core filled wholly by chains.) Here v is the space-filling ("van der Waals") volume associated with each molecule—it is an intrinsic property of each surfactant, independent of environment; hence $a^{(i)}$ and l_i are inversely related to one another, with proportionality constants v, $2v$, and $3v$ for bilayer, cylinder, and sphere packing, respectively. Note that for $i = 1$, l_i corresponds to a lamellar half-thickness, while for $i = 2$ and 3, it describes the rod and sphere radii.

As already mentioned, the $a_0^{(i)}$ can in principle be determined from an *a priori* formulation of the bulk free energies $g_i(a)$, i.e.,

we simply minimize $h_i(a) + g_i(a)$ with respect to a. From an information-theoretic point of view, for example, one can envisage calculating $g_i(a)$ via $P_i(\nu; a)$, the probability of conformation ν for a chain in environment i with head group area a; one could use as "input" here, say, the cubic lattice statistics of Dill and Flory (4). Alternatively, one can consider a machine simulation (5) in which specific choices are made for the bulk (e.g., chain conformational weights and interchain attraction and repulsion) contributions to the total energies of an i-environment molecule; the corresponding Boltzmann factors imply a free energy per surfactant which can be minimized with respect to l_i ($=iv/a_0^{(i)}$). Neither of these *a priori* approaches is very practical, however, since too little is known about the very complicated ingredients which lie at the heart of the compressional and splay elasticity of highly curved micelles. (For a discussion of these effects in the context of microemulsion-droplet bending energies, see Ref. (6).)

It is instructive nevertheless to consider the following form for $g_i(a)$:

$$g_i(l) = g_0^{(i)} + k_i(l - l_0^{(i)})^2, \qquad [7]$$

implying $g_i(a)$ via $l \leftrightarrow l_i = iv/a$. Recall that $g_i(l)$ is the free energy of an alkyl chain with length l (head group area iv/l) packed in environment i: $l_0^{(i)}$ is its optimum length, $g_0^{(i)}$ the corresponding minimum chemical potential, and k_i the associated elastic force constant. Because $k_i \neq 0$, adjusting l "all the way" to allow $iv/l = a_0$ (i.e., to optimize the head group situation) necessarily involves a free energy "price" "paid" by the tails. In general, then, l will adjust only partially, to affect a compromise (simultaneous) minimization of both $h_i(a)$ and $g_i(a)$ contributions to $\mu_i^0(a)$. The resulting $a_0^{(i)}$ and min $\tilde{\mu}_i^0$ will depend on the details of head group (γ, a_0) *and* tail (k_i, $l_0^{(i)}$) parameters. Again, the important point is that the final l_i ($\equiv iv/a_0^{(i)}$) is determined by chain elasticity as well as by surface energies.

In the theory of Israelachvili *et al.* (7) the chain free energy is considered only to the extent that l can never exceed a certain maximum value l_c which corresponds to the fully extended (all-*trans*) length. Thus for small enough a_0 it is concluded that only bilayer packing can be optimized, since $a_0 = 2v/l$ ($\equiv a_{cyl}$) or $3v/l$ ($\equiv a_{sph}$) would require $l > l_c$. But for larger a_0, e.g., $a_0 > 2v/l_c$, cylindrical packing can also be optimized; similarly for $a_0 > 3v/l_c$ all three environments can realize $a^{(i)} = a_0$, and there remains no criterion to distinguish between them.

Note that a common $a_0^{(i)} = a_0$ necessarily implies a common min $\mu_i^0(a) = \mu_{g=0}^0(a_0) = 2\gamma a_0$. But then there would be no incentive for a spherical micelle to grow into a rod or disk: $\tilde{\mu}_s^0$ would be constant for all s. More explicitly, consider a cylindrical micelle with globular ends where the cap radius (l_{cap}) is allowed to exceed that (l_{rod}) of the cylindrical "body." In this case the packing of surfactants in the caps is in general different from that in half- or full-spheres, i.e., $a_{cap} \leqslant 3v/l_{cap}$ and s_{cap} (= number of chains in the caps) is not constant—s_{cap} depends not only on l_{cap} but also on l_{rod}. Neglecting these complications for the moment, however, it is easy to show that

$$\tilde{\mu}_s^0 = 2\gamma a_0 + \alpha(1/s), \qquad [8]$$

where

$$\alpha = m\gamma a_0\left[\left(\frac{a_0}{a_{cap}}\right)^{1/2} - \left(\frac{a_{cap}}{a}\right)^{1/2}\right]^2$$

$$m = 4\pi l_{cap}^3/3v. \qquad [8A]$$

Here it has been assumed that $g_{rod}(a)$ is independent of a and hence that l_{rod} adjusts to give a_{rod} ($=2v/l_{rod}$) $= a_0$. To be consistent one should put $g_{cap}(a)$ equal to the the same constant; but then we would have $a_{cap} = a_0$, $\alpha = 0$, and spheres instead of rods! Instead, Israelachvili *et al.* (7) treat a_{cap} (and hence α) as a parameter to be fit to experimental data on rod aggregation numbers. They find $\alpha \simeq 30$ corresponding to $a_0/a_{cap} \simeq 3/4$ or $l_{cap} \gtrsim l_{rod}$. That is, a_{cap} is artificially prevented from achieving its optimum value (a_0), in order that large rods can be accounted for. We know though that, physically, what keeps a_{cap} from a_0 can only be the a-dependent part of $g_{cap}(a)$, the elasticity term which has been neglected.

(We have assumed here that a_0 is large enough so that $l < l_c$ is satisfied throughout the body and cap.)

Apart from the above ambiguities, another difficulty with setting $g_i \equiv$ constant and then letting $a^{(i)} \to a_0$ only in the body part of the micelle is that the possibility of rod/disk coexistence is precluded. More explicitly, instead of finite disks, a direct phase transition from monomers to a lamellar state ("infinite disks") is predicted (see Israelachvili *et al.* (7), and the "$y = 0$" cases presented below: here the finite disks are destabilized by too large a difference between the chemical potentials in the rim and body parts of the aggregate). This is in marked contradiction to recent experimental studies in which direct measurements of oblate micellar dimensions have been made. Charvolin *et al.* (8), for example, have used small-angle X-ray and neutron scattering spectra to infer disk anisotropies as small as 2–3:1 in the nematic state of potassium laurate/decanol/water. Furthermore, next to the discotic nematic phase of this system lies a "calamitic" phase consisting of comparably small-anisotropy rod-like micelles. There has also been reported a *biaxial* phase, sitting between these two, which most probably is composed of coexisting rods and disks (9). Strictly speaking, these experiments (see also the discussion of finite disks given in Ref. (10)) cannot be addressed directly by the present theory since they involve a *co*surfactant (viz. decanol) and hence *mixed* micelles. But the stability of finite disks has been established as well via similar measurements on *binary* systems, such as decylammonium chloride/water (with added salt) (11); see also the examples compiled in Ref. (2).

Let us return then to the likely scenario according to which the $g_i(a)$'s comprise a significant contribution to the $\tilde{\mu}_i^0(a)$'s. Then the optimum head group areas $a_0^{(i)}$ will be distinctly different from one another (and from a_0). This can be appreciated more concretely by rewriting Eq. [7] in the form

$$g_i(a) = [g + g_i^{(1)}] + g_i^{(2)}(1/a - 1/a_i^*)^2, \quad [7']$$

with $g + g_i^{(1)} \equiv g_0^{(i)}$, $g_i^{(2)} \equiv k_i i^2 v^2$, and $1/a_i^* = l_0^{(i)}/iv$. Here $g - \mu_1^0$ is the energy of transferring a chain from water into a liquid hydrocarbon environment, and a_i^* is the head group area which optimizes the bulk term $g_i(a)$. Note that $g_i(a_i^*) = [g + g_i^{(1)}]$ depends on i, and that the all-important $a_0^{(i)}$ from before is intermediate between a_i^* and a_0. This represents the head-tail coupling—the "compromise" optimization mentioned earlier—which is neglected in the usual treatments where $g_i(a)$ is approximated by the constant g. Similarly, the corresponding $\tilde{\mu}_i^0(a_0^{(i)}) \equiv \min \tilde{\mu}_i^0(a)$'s will vary with i.

Assuming that each $\tilde{\mu}_i^0(a)$ is optimized, i.e., adjusts to the appropriate $a_0^{(i)}$ in each environment of each micelle of interest, we can write, for example:

$$\tilde{\mu}_{s,\text{rod}}^0 = \tilde{\mu}_{\text{cyl,rod}}^0 + \frac{s_{\text{cap}}}{s}[\tilde{\mu}_{\text{cap}}^0 - \tilde{\mu}_{\text{cyl,rod}}^0] \quad [9]$$

and

$$\tilde{\mu}_{s,\text{disk}}^0 = \tilde{\mu}_{\text{cyl,disk}}^0 + \frac{s_{\text{rim}}}{s}[\tilde{\mu}_{\text{rim}}^0 - \tilde{\mu}_{\text{cyl,disk}}^0]. \quad [10]$$

Here $\tilde{\mu}_i^0 \equiv \min \tilde{\mu}_i^0(a) \equiv \tilde{\mu}_i^0(a_0^{(i)})$, where i = cyl, rod; cap; cyl, disk; and rim. s_{cap} and s_{rim} denote the number of surfactants in the caps of an s-rod and in the rim of an s-disk, respectively. Note that $\tilde{\mu}_{\text{cap}}^0$ (and obviously $\tilde{\mu}_{\text{cyl,rod}}^0$ and $\tilde{\mu}_{\text{cyl,disk}}^0$) and s_{cap} are independent of s, whereas $\tilde{\mu}_{\text{rim}}^0$ and s_{rim} depend on it in a very complicated way (see following section). Thus we must expect that there will be many surfactant/aqueous solution situations (i.e., many combinations of γ, c and $g_i(a)$'s) such that $\tilde{\mu}_{\text{cyl,rod}}^0 \simeq \tilde{\mu}_{\text{cyl,disk}}^0$ with $\tilde{\mu}_{s,\text{rod}}^0 - \tilde{\mu}_{s,\text{disk}}^0$ changing sign for not-too-large values of s. At the same time, since the rim and cyl, rod environments are so similar, we can have the quantity in square brackets in [10] small enough to suppress the monomer → bilayer transition. These situations imply crossover from, say, finite-disk to finite-rod dominance as the overall concentration (and hence $\bar{s}$) increases. In other cases, $\tilde{\mu}_{\text{cyl,rod}}^0/\tilde{\mu}_{\text{cyl,disk}}^0$ will differ enough from unity that one shape (rod or disk) will dominate at all concentrations. Quite generally,

then, the nature of the thermodynamic equilibrium depends on the relative and absolute magnitudes of the chemical potentials associated with each of the relevant surfactant environments.

In the present paper we describe a phenomenological theory of micelle shape and size which models the above spectrum of behaviors. Since too little is known about the actual elasticity effects which determine the $g_i(a)$ contributions discussed above, we choose to allow for them only indirectly as follows. We write $\tilde{\mu}_i^0(a) = \gamma a + c/a$ for all i and take l_i—the characteristic dimension of each environment—to also be fixed (l). As discussed earlier, this is essentially equivalent to what Israelachvili *et al.* (3, 7) have done. However, instead of setting $v/l = a_0$—or $2v/l = a_0$—we allow for intermediate cases in which

$$a_0 = \frac{v}{l}(1 + y) \qquad [11]$$

where $0 \leqslant y \leqslant 2$. l may be thought of as a mean of the l_i (spherical, hexagonal, lamellar) values associated with the surfactant in question. Similarly, a_0 represents an average of the optimum head group areas. The quantity y, then, "does the job" of the bulk elasticity effects which have been suppressed. It determines the relative stabilities of the several possible environments, just as the $\{g_i(a)\}$ fix the ordering of $\{\tilde{\mu}_i^0(a_0^{(i)})\}$. Thus, for example, $y = 0$ implies $a_{\text{cyl,disk}} = v/l = a_0$ and $a_{\text{cyl,rod}} = 2a_0$; hence $\tilde{\mu}^0(a) = \gamma a + c/a \equiv 2\gamma a_0 + \gamma a(1 - a_0/a)^2$ for cyl/rod ($\frac{5}{2}\gamma a_0$) will greatly exceed its value ($2\gamma a_0$) for cyl/disk, and rod-like micelles will not be able to compete. Conversely, $y = 1$ implies $\tilde{\mu}^0(a_{\text{cyl,disk}}) = \frac{5}{2}\gamma a_0 > \tilde{\mu}^0(a_{\text{cyl,rod}}) = 2\gamma a_0$, in which case disk-like micelles will not survive. But for intermediate values of $0 < y < 1$ we will have $\tilde{\mu}^0_{\text{cyl,rod}} \simeq \tilde{\mu}^0_{\text{cyl,disk}}$ with $\tilde{\mu}^0_{\text{rim}} - \tilde{\mu}^0_{\text{cyl,disk}}$ small and $\tilde{\mu}^0_{s,\text{rod}} - \tilde{\mu}^0_{s,\text{disk}}$ changing sign with s. (In fact, for $y = \sqrt{2} - 1$, $\tilde{\mu}^0_{\text{cyl,rod}}$ and $\tilde{\mu}^0_{\text{cyl,disk}}$ are identical (see algebra in Section II) thereby giving rise to the "crossover" from disk to rod (discussed in Section III.) Thus we recover the full spectrum of behaviors discussed in the preceding paragraph, where we considered explicitly the bulk elasticity contributions $[\{g_i(a)\}]$ to surfactant free energies.

In the following section we outline briefly our theory for rod-like and disk-like micelles. Recall that, once $\tilde{\mu}_i^0(a)$ is written in the form $\tilde{\mu}^0 = \gamma a + c/a$, $\tilde{\mu}_s^0$ follows directly from a specification of s_i and $a^{(i)}$:

$$\tilde{\mu}_s^0 = \frac{s_b}{s}\tilde{\mu}^0(a^{(b)}) + \frac{s_e}{s}\tilde{\mu}^0(a^{(e)}). \qquad [12]$$

Here s_b is the number of surfactants in the cylindrical body of an s-micelle, and $a^{(b)}$ is the corresponding head group area; similarly "e" (end) refers to surfactants in the cap (rod) and rim (disk) parts. Both the s_i's and $a^{(i)}$'s are determined straightforwardly by surface/volume geometric relations; only the latter quantities are dependent on the "y" parameter described above. Calculations of size distributions, based on the resulting expressions for $\tilde{\mu}_s^0$ (see Eq. [12]) are presented in Section III. We demonstrate there the possibility of rod/disk coexistence and discuss in detail the factors which control the relative importance of rods and disks. In the case of a surfactant/aqueous solution system characterized by $y \gtrsim 0$, for example, we find a monomer to infinite bilayer (lameallar phase) transition upon increasing the concentration. For larger y values ($y \leqslant \sqrt{2} - 1$), finite disks appear above the critical micelle concentration and grow—to the exclusion of rods—upon further concentration increases. For $y \simeq \sqrt{2} - 1$, rods and disks are found to be competitive, their relative importance varying with concentration—in particular, the disks give way to rods upon addition of soap. Then at higher y, rod-like micelles become dominant at *all* concentrations, both in number and size. Finally, for large enough y values ($y \gtrsim 1$), the rods give way to spheres. These several concentration behaviors, and their dependences on interfacial tension, are summarized and discussed critically. We also comment (in Section IV) on the connections between the present work and the earlier arguments of Tanford in which small disk-like micelles are featured.

II. ALGEBRA

A. Rods

We rewrite Eq. [9] in the more explicit form

$$\tilde{\mu}^0_{s,\mathrm{rod}} = \tilde{\mu}^0(a_{\mathrm{rod}}) + \frac{s_{\mathrm{cap}}}{s}[\tilde{\mu}^0(a_{\mathrm{cap}}) - \tilde{\mu}^0(a_{\mathrm{rod}})] \quad [13]$$

where $\tilde{\mu}^0(a)$ is given by head group terms alone:

$$\tilde{\mu}^0(a) = \gamma a_0\left(\frac{a}{a_0} + \frac{a_0}{a}\right) = 2\gamma a_0 + \gamma a\left(1 - \frac{a_0}{a}\right)^2. \quad [14]$$

Writing $m = 4\pi l^3/3v$ as before, and substituting $a_{\mathrm{rod}} = 2v/l$ and $a_{\mathrm{cap}} = 3v/l$ into Eqs. [13]–[14], it follows from $s_{\mathrm{cap}} = m$ and $a_0 = (v/l)(1 + y)$ that

$$\tilde{\mu}^0_{s,\mathrm{rod}} = \tilde{\mu}^0_{\infty,r} + \alpha_r \frac{1}{s} \quad [15]$$

where

$$\tilde{\mu}^0_{\infty,r} = 2\gamma a_0\left[1 + \frac{(1-y)^2}{4(1+y)}\right] = \tilde{\mu}^0(a_{\mathrm{rod}}) \equiv \tilde{\mu}^0_{\mathrm{cyl,rod}} \quad [15A]$$

and

$$\alpha_r = \frac{m\gamma a_0}{6(1+y)}(5 - 2y - y^2). \quad [15B]$$

Note that the $a_{\mathrm{cap}} = \frac{3}{2}a_0$ ($l_{\mathrm{cap}} = l_{\mathrm{rod}}$) limit of Eq. [8] corresponds to the $a_{\mathrm{cap}} = \frac{3}{2}a_0$ ($y = 1$) limit of Eq. [15].

B. Disks

Just as our rod-like micelle was taken to be a spherocylinder, i.e., a prolate right-circular cylinder with half spherical caps, our disk is modeled by an oblate right-circular cylinder "closed" by a half-toroidal rim. Rewriting Eq. [10] as (here $a_{\mathrm{disk}} = v/l = a_0/(1 + y)$)

$$\tilde{\mu}^0_{s,\mathrm{disk}} = \tilde{\mu}^0(a_{\mathrm{disk}}) + \frac{s_{\mathrm{rim}}}{s}[\tilde{\mu}^0(a_{\mathrm{rim}}) - \tilde{\mu}^0(a_{\mathrm{disk}})], \quad [16]$$

we need only determine a_{rim} and s_{rim} as explicit functions of v, l, and s. Equating sv to the volume of a disk-like micelle, we have

$$sv = \frac{\pi d_s^2 l}{2} + \frac{\pi^2 d_s l^2}{2} + \frac{4}{3}\pi l^3, \quad [17]$$

where d_s is the diameter of the right-circular cylinder ("flat") part and l is its half-thickness. Solving for d_s in Eq. [17] gives

$$d_s = \left(\frac{2v}{\pi l}\right)^{1/2}\left[s + m\left(\frac{3\pi^2}{32} - 1\right)\right]^{1/2} - \frac{\pi l}{2}. \quad [18]$$

Note that the first term in [17] is simply the volume of the flat part of the micelle; it follows then from $s_{\mathrm{flat}}v = (s - s_{\mathrm{rim}})v = \pi d_s^2 l/2$, and Eq. [18] for d_s, that

$$s_{\mathrm{rim}} = \frac{\pi}{2}\left(\frac{3m}{2}\right)^{1/2}\left[s + m\left(\frac{3\pi^2}{32} - 1\right)\right]^{1/2} - m\left(\frac{3\pi^2}{16} - 1\right). \quad [19]$$

Finally, recognizing that $s_{\mathrm{rim}}a_{\mathrm{rim}} = \pi^2 d_s l + 4\pi l^2$ = area of rim in an s-micelle, we have

$$a_{\mathrm{rim}} = \frac{v}{l}\left(2 + \frac{m}{s_{\mathrm{rim}}}\right) = \frac{a_0}{1+y}\left(2 + \frac{m}{s_{\mathrm{rim}}}\right). \quad [20]$$

Substituting Eqs. [19]–[20] into Eq. [16] gives

$$\tilde{\mu}^0_{s,\mathrm{disk}} = \tilde{\mu}^0_{\infty,\mathrm{d}} + \alpha_{\mathrm{d}} f_{\mathrm{d}}(s), \quad [21]$$

with

$$\tilde{\mu}^0_{\infty,\mathrm{d}} = 2\gamma a_0\left[1 + \frac{y^2}{2(1+y)}\right] = \tilde{\mu}^0(a_{\mathrm{disk}}) = \tilde{\mu}^0_{\mathrm{cyl,disk}} \quad [21A]$$

$$\alpha_{\mathrm{d}}(s) = \left(\frac{3m}{32}\right)^{1/2}\frac{\pi\gamma a_0}{1+y} \times \left[1 - \frac{y(2+y)}{1 + \dfrac{m}{s_{\mathrm{rim}}}}\right], \quad [21B]$$

and

$$f_{\mathrm{d}}(s) = \left(\frac{32m}{3\pi^2}\right)^{1/2}\frac{1}{s}\frac{(1 + s_{\mathrm{rim}}/m)^2}{(1 + 2s_{\mathrm{rim}}/m)}. \quad [21C]$$

Note that, in comparing [21] with [15] $\alpha_{\mathrm{d}}(s) \to$ constant *only as* $s \to \infty$; in this same limit,

$f_d(s) \to 1/\sqrt{s}$ (vs $1/s$). Much is made of these differences in the discussion of Section III.

C. Coexistence

Denote by $x_{s,\text{rod}}(x_{s,\text{disk}})$ the mole fraction of surfactant incorporated into rods (disks) with aggregation number s. Then the total concentration can be conveniently expressed as

$$X = x_1 + x_r + x_d = x_1 + \sum_{s\geq m} x_{s,\text{rod}} + \sum_{s\geq m} x_{s,\text{disk}}, \quad [22]$$

and number and weight averages defined as

$$\bar{S}_{N_{r(d)}} = \frac{[x_1 + \sum x_{s,\text{rod(disk)}}]}{\left[x_1 + \sum \frac{1}{s} x_{s,\text{rod(disk)}}\right]} \equiv \frac{1}{\left\langle \frac{1}{s} \right\rangle_{r(d)}} \quad [23]$$

and

$$\bar{S}_{w_{r(d)}} = \frac{[x_1 + \sum s x_{s,\text{rod(disk)}}]}{[x_1 + \sum x_{s,\text{rod(disk)}}]} \equiv \langle s \rangle_{r(d)}. \quad [24]$$

Returning to Eqs. [4] and [15] it is straightforward to show that

$$x_r = e^{-\alpha_r}\left\{\frac{m(x_1 A_r)^m}{1 - x_1 A_r} + \frac{(x_1 A_r)^{m+1}}{(1 - x_1 A_r)^2}\right\} \quad [25]$$

with

$$A_r = e^{\beta(\mu_1^0 - \tilde{\mu}_{\infty,r}^0)} \quad [26]$$

and that

$$\bar{S}_{N_r} = \frac{x_1 + x_r}{x_1 + \frac{e^{-\alpha_r}(x_1 A_r)^m}{1 - x_1 A_r}} \quad [27A]$$

and

$$\bar{S}_{w_r} = \frac{x_1 + x_r\left[m + \frac{x_1 A_r}{1 - x_1 A_r}\left\{1 + \frac{1}{m(1 - x_1 A_r) + x_1 A_r}\right\}\right]}{x_1 + x_r}. \quad [27B]$$

For x_d, $\bar{S}_{Nd}$, and $\bar{S}_{wd}$ it is no longer easy to obtain closed-form expressions. One can, however, simply perform numerical computations based on Eqs. [4], [21] and the definitions of the x's and $\bar{s}$'s to determine all of these quantities.

More explicitly, in the case of disks, say we start by choosing a reasonable set of values for γ, $a_0(y)$, v, l, and μ_1^0 (see the first paragraph of the following section). This allows us to evaluate $\tilde{\mu}_{s,\text{disk}}^0$ (see Eq. [21] with s_{rim} given by Eq. [19] and $m = 4\pi l^3/3v$) for each $s \geq m$. The size distribution $x_{s,\text{disk}} = s x_1^s \exp\{s\beta(\mu_1^0 - \tilde{\mu}_{s,\text{disk}}^0)\}$ can then be calculated for each monomer concentration x_1, with x_d and the $\bar{s}_d$'s following from Eqs. [22]–[24]. For large enough y (see discussion in Section III) a value of x_1 is reached (*before* $x_1 = 1/A_d$) above which $x_d \gg x_1$, i.e., the molecules are essentially completely micellized into disk-like aggregates.

In the case of rods we can follow an analogous procedure for the *same* set of values for γ, a_0, v, l, and μ_1^0—we wish to treat, afterall, the same surfactant, under identical solution conditions, in an effort to describe the equilibrium coexistence between different sizes *and shapes* of micelles. That is, we evaluate $\tilde{\mu}_{s,\text{rod}}^0$ according to Eq. [15] and hence $x_{s,\text{rod}} = s x_1^s \exp\{s\beta(\mu_1^0 - \tilde{\mu}_{s,\text{rod}}^0)\}$ and x_r (and the $\bar{s}_r$'s) for each x_1. (Equivalently we can solve Eqs. [25] and [27] directly.) Then, with the neglect of intermicelle interactions, we need only superpose these results on those obtained in the disk case. Since rods and disks will be in equilibrium with each other if they coexist with the same monomer concentration, we can simply collect the $\{x_{s,\text{rod}}\}$ and $\{x_{s,\text{disk}}\}$ corresponding to common x_1 values: $x_{\text{total}} \equiv X = x_1 + \Sigma\, x_{s,\text{rod}} + \Sigma\, x_{s,\text{disk}}$.

III. Numerical Results and Discussion

There has been much controversy in the recent literature about how to choose a reasonable value for the interfacial tension γ. Israelachvili *et al.* (7) have argued that it should

be as large as 50 erg/cm^2, the familiar value appropriate to an "unadulterated" hydrocarbon–water interface; Tanford (2) and Jönsson and Wennerström (12) and others have concluded, however, that it should be regarded as two to three times smaller. Since the present discussion is not affected qualitatively by the specific choice of γ, we shall start with values in the range 15–25 erg/cm^2. For the molecular constants characterizing an individual surfactant we take: μ_1^0, the isolated monomer free energy, to be $15kT$; v the volume of an amphiphilic chain, to be 360 Å^3 and l, the average characteristic dimension of a micelle, to be 12 Å. These are all consistent with typical values cited, say, in Tanford's monograph. Note that m, the minimum micelle number, follows from l and v via $m = 4\pi l^3/3v$. Similarly, the optimum head group area a_0 is determined by the choice of $0 \leqslant y \leqslant 1$ according to $y = (l/v)a_0 - 1$.

Intuitively one might expect that $a_0 = v/l \equiv a_d$ (=30 Å^2 in our case), i.e., $y \equiv 0$—should lead to the formation of disks, whereas $a_0 = 2v/l \equiv a_r$ (=60 Å^2)—$y \equiv 1$ favors the dominance of rods. But, because of "end effects" (i.e., the half-toroidal rings "closing" the disks and the half-spherical caps on the rods), this is not seen to be the case. Rods and disks form only when y is greater than 0.35 and less that $\simeq$0.80; otherwise they give way to bilayers and spheres, respectively.

For γ as small as 15 ergs/cm^2 we find that the micelles remain small, i.e., with weight average aggregation numbers less than 100, up through total concentrations as large as 5×10^{-3}. For $X > 5 \times 10^{-3}$ the volume ($\simeq$weight) fraction of surfactant exceeds several per cent and we are no longer dealing with a dilute solution. In a recent communication (13), in fact, we have shown that average sizes are already significantly affected by the inter-micelle interaction at $X > 5 \times 10^{-3}$.

For $\gamma \simeq 21$ ergs/cm^2 we find larger micelles, with the details of size and shape depending sensitively on X and y. For $y \leqslant 0.4$ no micellization occurs for x_1 less than $1/A_d$. (Note that $1/A_d < 1/A_r$ for $y < \sqrt{2} - 1$; this follows directly from Eqs. [26] and [26; r $\rightarrow$ d] for A_r and A_d.) The reason for this has been pointed out by Israelachvili *et al.* (7) and by Wennerström (14), and is discussed further below. When x_1 finally achieves the value $1/A_d$, i.e., $\tilde{\mu}_{\infty,d} = \mu_1^0 + kT \ln x_1$, a phase transition occurs from monomer to bilayer. With no micellization taking place, then, we have that x_1 increases with total concentration according to $x_1 = X$; at $x_1 = X = 1/A_d$ a lamellar phase appears and x_1 thereby remains constant ($=1/A_d$) as X grows further.

For $y \gtrsim 0.40$ a threshold for formation of finite aggregates is observed. For $0.40 \leqslant y \leqslant 0.43$ the number of disk-like micelles greatly exceeds that of rods; for larger y values the reverse is true. This fact is displayed in Table I where the ratio x_d/x_r is seen to invert at $y \simeq 0.43$. At a concentration of $X \simeq 3 \times 10^{-4}$, for example, x_d/x_r falls from $\simeq$10 to $\simeq$1 to $\simeq$0.1 as y increases from $\simeq$0.414 to $\simeq$0.430 to $\simeq$0.500. For $y \simeq 0.43$, where rods and disks coexist most nearly in comparable number, an increase in total concentration has the effect of favoring rods over disks: $X \simeq 3.5 \times 10^{-4} \rightarrow 5.0 \times 10^{-3}$ leads to $x_d/x_r = 1.2 \rightarrow 0.6$.

The control of micellar shape via overall concentration of surfactant can be understood as follows. Figure 1 shows the dependence of $\tilde{\mu}_s^0$ on s for rods and disks. Most important is the fact that $\tilde{\mu}_s^0$ decreases faster for disks than for rods when $s \gtrsim m$. Recall from Eq. [15] that $\tilde{\mu}_{s,\text{rod}}^0$ decreases as $1/s$ *for all* s; $\tilde{\mu}_{s,\text{disk}}^0$, on the other hand, decreases *faster* than $1/s$ for $s \gtrsim m$ (the explicit s-dependence is quite complicated, see Eq. [21]) and *slower* than $1/s$ ($\sim 1/\sqrt{s}$ for $s \gg m$) at large s. That is, as we leave the minimum micelle (sphere limit), it is at first best to grow in *two* rather than *one* dimension: the disk is preferred over the rod because surfactants in the quasi-cylindrical rim enjoy a lower chemical potential than those in the spherical caps. But then as s increases significantly beyond m, the rod becomes preferable because its "end molecules" are more efficiently rendered a minority. For $s \simeq 400$, for example, we have $s_{\text{rim}} \simeq 155$ as opposed to s_{cap} ($=m$) $\simeq 20$. Accordingly, since $\tilde{\mu}_{\infty,r}^0$

TABLE I

Number and Weight Averages of Micelles in the Surfactant–Water System[a]

x_d/x_r	y	X_{total} ($\times 10^4$)	x_r ($\times 10^4$)	x_d ($\times 10^4$)	$\bar{S}_{N_r}, \bar{S}_{w_r}$	$\bar{S}_{N_d}, \bar{S}_{w_d}$
—	0.35	2.0	0	0	1.0, 1.0	1.0, 1.0
168	0.40	3.04	0.0164	2.76	5.3, 1.1	11, 405
11	$\sqrt{2}-1$	3.36	0.272	2.98	1.4, 42	11, 187
54	$\sqrt{2}-1$	49.6	0.897	48.7	4.2, 322	118, 518
1.2	0.43	3.51	1.46	1.78	6.0, 399	6.8, 106
0.06	0.43	50.3	47.3	3.06	149, 2690	9.0, 123
0.13	0.50	3.26	2.57	0.334	8.4, 336	2.0, 27
0.01	0.50	49.6	48.8	0.448	126, 1640	2.3, 30
0.21	0.60	3.44	2.51	0.523	6.7, 152	2.2, 21
0.01	0.60	50.7	49.5	0.732	92, 759	2.6, 25
1.1[b]	0.80[b]	3.40	1.29	1.46	2.8, 27	3.0, 20
0.17	0.80	50.3	42.3	7.24	36, 134	8.5, 28
1.7[b]	1.00[b]	3.40	0.888	1.51	1.8, 12	2.4, 15
1.3[b]	1.00[b]	50.1	21.8	27.5	12, 32	13, 26

[a] v = 360 Å^3, l = 12 Å, γ = 21 ergs/cm^2, $\mu_1^0 = 15kT$.

[b] Note that for these concentrations and values of y, the number and weight averages are not large enough to indicate the presence of either anisotropic rods or disks. The micelles formed resemble distorted spheres.

$\approx \tilde{\mu}^0_{\infty,d}$ whereas $\tilde{\mu}^0_{rim} > \tilde{\mu}^0_{\infty,r}$, it follows that $\tilde{\mu}^0_{s,rod} \simeq \tilde{\mu}^0_{\infty,r} < \tilde{\mu}^0_{s,disk} \approx \tilde{\mu}^0_{\infty,r} + s_{rim}/s(\tilde{\mu}^0_{rim} - \tilde{\mu}^0_{\infty,r})$ at large s—the disk gives way to the rod. From Fig. 1 we see that this occurs for $s \gtrsim 200$ for the particular choice of molecular parameters considered here. (The above discussion pertains specifically to $y \simeq 0.43$.)

The fact that $\tilde{\mu}^0_{s,disk}$ passes over $\tilde{\mu}^0_{s,rod}$ for intermediate values of s necessarily implies a crossover from disk to rod dominance as the concentration is increased. This is because in general (i.e., suppressing the details of the s-dependences of chemical potentials for different micellar shapes) *average aggregation numbers increase with overall concentration,* as long as $\tilde{\mu}^0_s$ decreases with s. Thus, increasing X moves us through the crossover region in Fig. 1 from left to right. That is we pass from typical s values being less than 400, say, to ones which are significantly greater; correspondingly we switch over from smallish disks to largish rods. This is seen in the $y \simeq 0.43$ entry of Table I which shows a change from $\bar{s}_w \simeq 100$ disks to $\bar{s}_w \simeq 2700$ rods as X is increased from 3.5×10^{-4} to 5.0×10^{-3}.

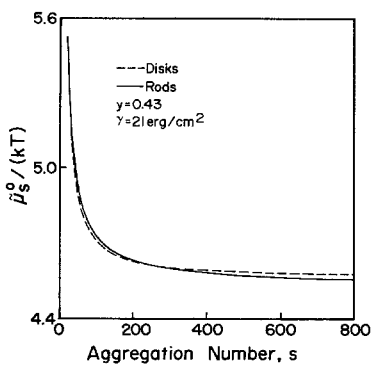

FIG. 1. Standard chemical potential per surfactant in a micelle as a function of the micelle aggregation number: v = 360 Å^3, l = 12 Å, $\mu_1^0 = 15kT$, γ = 21 ergs/cm^2, and y = 0.43.

This switchover in size and shape can be seen from another point of view in Fig. 2. Here we plot the size distributions for disks and rods for the two total concentrations mentioned above. At 3.5×10^{-4} (see Fig. 2A) the majority of surfactant molecules are incorporated in disk-like aggregates, with a relatively narrow distribution peaked near $s \simeq 90$; the more broadly dispersed rods show a most probable value of $s \simeq 250$. At $X \simeq 5.0 \times 10^{-3}$ (Fig. 2B) however, the disks have become outnumbered by rods: $x_r/x_d \equiv (\sum_{s \gtrsim m} N_{s,rod})/(\sum_{s \gtrsim m} N_{s,disk})$ is as large as 15.

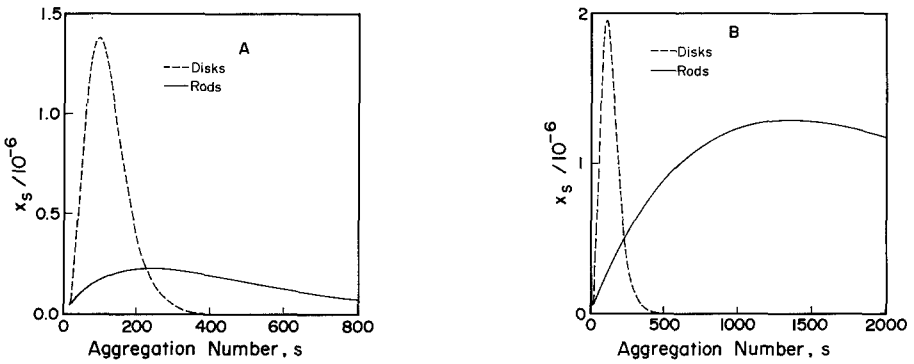

FIG. 2. Distributions of rods and disks at two different overall surfactant concentrations: (A) $X = 3.51 \times 10^{-4}$, $\bar{s}_{N_r} = 6.0$, $\bar{s}_{w_r} = 399$, $\bar{s}_{N_d} = 6.8$, and $\bar{s}_{w_d} = 106$; (B) $X = 5.03 \times 10^{-3}$, $\bar{s}_{N_r} = 149$, $\bar{s}_{w_r} = 2690$, $\bar{s}_{N_d} = 9.0$, and $\bar{s}_{w_d} = 123$. The molecular parameters here are the same as in Fig. 1.

(Here $N_{s,\text{rod}}$ is the number of amphiphiles ("monomers") incorporated into rods of size s.) Also, the disk distribution has simply shifted over slightly—the peak position adjusting from $\simeq$90 to $\simeq$100. The rods, on the other hand, have had their $s_{\text{most probable}}$ increase from $\simeq$250 to $\simeq$1300. This again heralds the crossover, with increasing concentration, from small disks to larger rods when y assumes intermediate ($\simeq$0.43) values.

We comment now on several other behaviors of micellar growth which are evidenced in Table I.

(i) For $0 \leqslant y \leqslant 0.4$, no micellization occurs. This is because a phase transition from monomer to bilayer intervenes. More explicitly, it is straightforward to show from the analysis in Section II.B that the size distribution of disks is given by

$$x_s = s(x_1 A_d)^s e^{-s\beta\alpha_d(s) f_d(s)} \qquad [28]$$

where for large s

$$\alpha_d(s) \rightarrow \text{constant} = \left(\frac{3m}{32}\right)^{1/2} \pi\gamma a_0 (1 - 2y - y^2)/(1 + y) \qquad [21B']$$

and

$$f_d(s) \rightarrow \frac{1}{\sqrt{s}} \qquad [21C']$$

(As before, $A_d \equiv e^{\beta(\mu_1^0 - \tilde{\mu}_{\infty,d}^0)}$. Note that α_d (large s) is a strongly decreasing function of y, while it is directly proportional to γ. Thus, for any combination of small enough y and sufficiently big x_1, the sum $\sum_{s \geqslant m} x_{s,\text{disk}}$ will remain negligible compared to x_1 no matter how closely $x_1 A_d$ approaches 1. Then, for $x_1 = 1/A_d$ a bilayer appears since it can now be in equilibrium with monomer, i.e., $x_1 = 1/A_d = e^{-\beta(\mu_1^0 - \tilde{\mu}_{\infty,d}^0)}$ is equivalent to $\tilde{\mu}_{\infty,d}^0 = \mu_1^0 + kT \times \ln x_1$. At this point $\sum_{s \geqslant m} x_{s,\text{disk}} = \sum_{s \geqslant m} \times s e^{-\alpha_d(s) f_d(s)} \ll x_1$, corresponding to a virtual absence of finite disks. Rods are also excluded, since they cannot appear before x_1 reaches a value close to (but necessarily less than) $1/A_r = e^{-\beta(\mu_1^0 - \tilde{\mu}_{\infty,r}^0)}$, and $1/A_r > 1/A_d$ for $0 \leqslant y \leqslant 0.4$. Furthermore, *infinite* rods (i.e., via transitions to the hexagonal phase) are not possible since this would require $x_1 A_d = 1$ thereby implying a divergence in mole fraction:

$$X \equiv x_1 + x_d + \sum_{s \geqslant m} s e^{-\alpha_r} = \infty$$

the sum blowing up since α_r is independent of s for all s.

In summary, then, as pointed out earlier by Israelchvili *et al.*[7] and by Wennerstrom (14), micellization involving finite aggregates will be suppressed by a direct monomer $\rightarrow$ bilayer transition whenever α_d is large enough, i.e., whenever bilayer packing is sufficiently strongly favored over others. Note that $\alpha_d(s)$ is indeed a measure of the chemical potential difference between the "rim" (curved) and

"body" (flat) parts of a disk-like micelle containing s amphiphiles. And the fact that α_d decreases sharply with y explains why we do not see finite aggregates until y is as large as 0.35 (γ = 15 ergs/cm^2) or 0.40 (γ = 21 ergs/cm^2); that y_{min} increases with interfacial tension is an immediate consequence of $\alpha_d \sim \gamma$. Similarly, the prediction of Israelachvili *et al.* that finite disks are overwhelmed by the bilayer phase follows directly from the choice of $y = 0$ and γ = 50 ergs/cm^2. In the present case, finite disks appear as a result of our larger y and smaller γ and because $\tilde{\mu}^0_{s,disk}$ has been allowed to decrease faster than $1/s$ for $s \gtrsim m$ (see Eq. [21]) rather than being forced to fall off according to its asymptotic ($s \gg m$) form $(1/\sqrt{s})$; we return to these points in the discussion of Section IV.

(ii) Disk size decreases with y. In the above we have treated the $s \to \infty$ limit of $\alpha_d(s)$ as a measure of the driving force for growth of disks; from Eq. [21B] we saw that it was a strongly decreasing function of y. Similarly, we can consider the fractional change $\Delta_d \equiv [(\tilde{\mu}^0_m - \tilde{\mu}^0_{\infty,d})/\tilde{\mu}^0_{\infty,d}]$ as an index of the disk's tendency to grow. From Eq. [21] it is easy to show that Δ_d decreases by almost 50% as y is raised from 0.4 to 0.5. Correspondingly we expect a dramatic decrease in micellar size over this small range of y for which disks are important.

Indeed, for $X \simeq 3 \times 10^{-4}$, Table I shows that the weight average aggregation number plummets from 405 to 187 to 106 to 27 as y increases from 0.40 to 0.414 to 0.43 to 0.50.

(iii) Disks give way to rods for intermediate y. In the beginning of this section we have already mentioned that an inversion of x_d/x_r (micellar shape preference) occurs at $y \gtrsim \sqrt{2} - 1$, and we have discussed this behavior via annotation of Figs. 1 and 2.

(iv) Rod size decreases with y. In analogy with the discussion in (ii) above we can define a rod growth parameter by $\Delta_r \equiv [(\tilde{\mu}^0_m - \tilde{\mu}^0_{\infty,r})/\tilde{\mu}^0_{\infty,r}]$ and show from Eq. [15] that Δ_r decreases with y according to $(5 - 2y - y^2)/(5 + 2y + y^2)$. Equivalently, we have directly from Eq. [15B] that the coefficient α_r decreases as $(5 - 2y - y^2)/(1 + y)$. (Recall that in the case of rods we can write $\tilde{\mu}^0_{s,rod} = \tilde{\mu}^0_{\infty,r} + \alpha_r/s$, with α_r = constant *for all s.*) Consistent with this, Table I shows a dramatic decrease in micellar size as y runs through the range for which rods are able to compete: $\bar{s}_{w,rod}(\bar{s}_{N,rod})$ falls off from 2690 (400) to 1640 (340) to 760 (150) as y is increased from 0.43 to 0.5 to 0.6. Equivalently we can account for the growth of rods observed by Mazer *et al.* (15) upon addition of salt—the electrolyte screens the head group repulsions, thereby decreasing a_0 and hence y.

(v) Spherical micelles predominate as y ≳ 1. The α_r discussed above, equal (see Eq. [15B]) to $m\gamma a_0(5 - 2y - y^2)/6kT(1 + y)$ can also be expressed as m times the difference in chemical potentials between surfactants in the "cap" and "body" parts of the rod. Thus, for large enough y and small enough γ, the lowering of $\tilde{\mu}^0_s$ achieved via growth is no longer sufficient to offset the loss of mixing entropy attendant upon having fewer (and larger) micelles. Accordingly, spherical ($s \gtrsim m$, minimum size) aggregates will become the predominant species. This is seen in Table I, whose $y \gtrsim 0.8$ entries describe essentially spherical micelles ($\bar{s} \simeq m$); here the distinction between rod and disk shapes loses its meaning (as do consequently the x_d/x_r ratios, etc.).

IV. SUMMARY

To summarize our results on the relative stability of rods and disks, recall the spectrum of headgroup areas shown in Fig. 3A. At the same time, consider the dependence of μ^0 and a, shown schematically in Fig. 3B.

(1) As discussed in the Introduction, Israelachvili *et al.* (7) argue that—in order to have rod-like or disk-like aggregation—l adjusts "all the way" to give $2v/l = a_0$ or $v/l = a_0$. It follows that a in the "ends" must be at least three-halves its (optimum, a_0) value in the "body:" more explicitly, for $a_{cyl,rod} = 2v/l = a_0$ ("$y = 1$") one has $a_{end} = 3v/l = (3/2)a_0$, whereas for $a_{cyl,disk} = v/l = a_0$ ("$y = 0$") $a_{end} = (2 + m/s_{rim})v/l \gtrsim 2a_0$. [Here we have as-

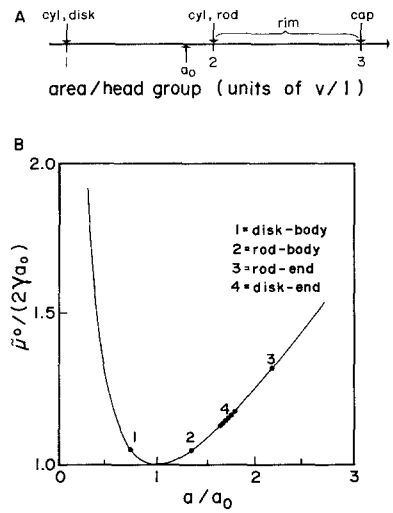

FIG. 3. Head group areas and chemical potentials per surfactant in the various micellar environments: (A) Head group areas relative to a_0; (B) Chemical potential per surfactant relative to $\mu^0(a_0) = 2\gamma a_0$ for $y = \sqrt{2} - 1$.

sumed that l in the "ends" (cap, rim) is the same l as in the "bodies" (cyl, rod and cyl, disk).] Thus the free energy μ^0 of molecules in the ends is necessarily much higher than that of surfactants in the bodies. For rods this means large α_r (see Eq. [15B] with $y = 1$) and consequently large $\bar{s}_w \simeq 2\sqrt{x}e^{\alpha_r/2}$.

For disk-like aggregation, on the other hand, the treatment of Israelachvili *et al.* corresponds to putting $y = 0$; employing a γ value more than twice the one used here; and taking the large s ($s \to \infty$, $1/\sqrt{s}$) fall-off of $\tilde{\mu}^0_{s,\text{disk}}$ to apply for small s as well. As a consequence of these choices, the rims involve an intolerably high μ^0 compared to the (fully optimized) value in the body. Recall that $s_{\text{rim}} = \mathcal{O}(\sqrt{s})$, i.e., the rim molecules always make a significant contribution to the weighted-sum chemical potential $\tilde{\mu}^0_{s,\text{disk}}$. Furthermore,

$$\tilde{\mu}^0_{s,\text{disk}} - \tilde{\mu}^0_{\infty,\text{d}} = \mathcal{O}\left[\alpha_{\text{d}}(\infty)\frac{1}{\sqrt{s}}\right],$$

with $\alpha_{\text{d}}(\infty)$ decreasing strongly with y—in particular, as $(1 - 2y - y^2)/(1 + y)$ (cf. Eq. [21B]). Accordingly, the choice of $y = 0$ (against, say, $y \simeq \sqrt{2} - 1$) leads to an $\alpha_{\text{d}}(\infty)$ which is from one to two orders of magnitude larger than ours and to the prediction that a monomer → bilayer transition occurs before micellization into finite disks becomes possible.

The present $0 < y < 1$ theory allows directly for smaller differences between μ^0_{body} and μ^0_{end}, i.e., for smaller values of $\tilde{\mu}^0_{s,\text{d}} - \tilde{\mu}^0_{\infty,\text{d}}$ for all s. As described in the introduction, this situation arises from the chain elasticity effects which are generally neglected. Consider, for example,

$$a_0 = \frac{v}{l}(1 + y)$$

with $y \simeq \sqrt{2} - 1$. Then we have $a_{\text{cyl,disk}} \equiv v/l \simeq (1/\sqrt{2})a_0$, $a_{\text{cyl,rod}} \equiv 2v/l \simeq \sqrt{2}a_0$, $a_{\text{cap}} \equiv 3v/l \simeq (3/\sqrt{2})a_0$ and $a_{\text{rim}} \simeq (2 \leftrightarrow 3/\sqrt{2})a_0$ corresponding to the four sets of points labelled by "1", "2", "3", and "4" in Fig. 3B; this is equivalent to taking $\mu^0(a)$ just below μ^0 ($2v/l \equiv a_{\text{cyl,rod}}$) (see Figs. 3A and B) with $a_0 \equiv (1 + y)v/l \simeq (1/\sqrt{2})a_{\text{cyl,rod}}$. In this case we note that α_r [$\sim(\mu^0_{\text{end}} - \mu^0_{\text{body}})_{\text{rod}}$ = ("3" − "2")] and hence $(\bar{s}_w)_{\text{rod}}$ are larger than for $y = 1$, the optimized rod situation. But, more interestingly, α_{d} [$\sim$("4" − "1")] is significantly (one-to-two orders of magnitude, as mentioned above) *smaller* than in the disk-optimized $y = 0$ case. As a result, the finite disks become competitive with bilayers as outlined in the discussion of Section III (ii).

Note that, in the above, the difference between chemical potentials of molecules in the rim and body of a disk has been made small by taking a_0 intermediate between $a = v/l$ and $a = 2v/l$ (i.e., $0 < y < 1$ (see again Figs. 3A and B)). As stressed earlier in the Introduction this is phenomenologically equivalent to including explicitly the chain elasticity contributions, i.e., to putting

$$\mu^0(a) = \gamma\left(a + \frac{a_0^2}{a}\right)$$

$$\to \mu_i^0(a) = \gamma\left(a + \frac{a_0^2}{a}\right) + g_i(a)$$

and optimizing (minimizing) the *total* $\mu_i^0(a)$ for each i. The optimum head group area

$a_0^{(i)}$ is now different for each environment, increasing from "cyl, disk" to "cyl, rod" to "rim" to "cap." This makes possible small differences in standard chemical potentials $\mu_i^0(a)$, because $a^{(i)}_{\text{"packing"}} = iv/l$ increases in the same order. In the "usual" treatments, on the other hand, a common a_0 is assumed for all i, and $a^{(i)}_{\text{packing}} = iv/l$ is set equal to a_0 (via adjustment of the common l) for $i = 1$ *or* 2; as a consequence, all chemical potential differences ("end"–"body") are necessarily large.

(2) The treatment of Tanford (2) can be related to the present formulation, as follows. He describes a situation where $a_{\text{cyl,disk}}$ is markedly smaller than the optimal head group area a_0; this corresponds to our y being significantly greater than zero. Recall that we have computed $\tilde{\mu}_s^0$ as a weighted sum of $\tilde{\mu}^0_{\text{cyl,disk}}$ and $\tilde{\mu}^0_{\text{rim}}$, the chemical potentials for molecules in the two micellar environments: $\tilde{\mu}^0_{s,\text{d}} = (s - s_{\text{rim}}/s)\tilde{\mu}^0_{\text{cyl,d}} + (s_{\text{rim}}/s)\tilde{\mu}^0_{\text{rim}}$, with $\tilde{\mu}_i^0 \equiv \tilde{\mu}^0(a_i)$ and $\tilde{\mu}^0(a) = \gamma a + a_0^2\gamma/a$. In an essentially equivalent scheme, Tanford computes a_s as a weighted sum of a_i: $a_s = (s - s_{\text{rim}}/s)a_{\text{cyl,d}} + (s_{\text{rim}}/s)a_{\text{rim}}$, with $\tilde{\mu}_s^0$ following from $\tilde{\mu}^0(a_s)$.[2] The key point is that his choice of molecular parameters and of $\mu^0(a)$ dependence leads to an a_0 value which is conspicuously greater than $a_{\text{cyl,disk}} = v/l$. In the case of SDS in 0.1 *M* NaCl, for example, he has the minimum in $\mu^0(a)$ occurring at $a \simeq 75$ Å$^2 = a_0$, with $a_{\text{cyl,disk}} \simeq 26$ Å^2, $a_{\text{cyl,rod}} \approx 68$ Å^2, $a_{\text{cap}} \simeq 132$ Å^2, and $a_{\text{rim}} \simeq 132 - 68$ Å^2 [$s = 24$ ($=m$) $\rightarrow \infty$]. Thus, as in our $0 < y < 1$ theory, neither $a_{\text{cyl,disk}}$ *nor* $a_{\text{cyl,rod}}$ is optimized to a_0. Instead we have a situation in which

at small s (<250)—where a large fraction of molecules are in the "ends"—disk-like micelles are preferred because rod-like ones pay too high a μ^0 "price" in their caps ($a_{\text{cap}} \simeq 132 \gg 75$ Å$^2 \simeq a_0$, as opposed to $a_{\text{rim}} \simeq 89$–79 Å^2 for $s \simeq 100 \rightarrow 250$), and

at large s—where the "bodies" dominate—rod-like micelles are more stable since $a_{\text{cyl,rod}} \simeq 68$ Å$^2 \leqslant a_0$ compared to $a_{\text{cyl,disk}} \simeq 26$ Å$^2 \ll a_0$.

The above scenario is consistent with the situation shown in Fig. 3A, in which $a_{\text{cyl,rod}}$, $a_{\text{rim}} \simeq a_0$ and $a_{\text{cyl,disk}} \ll a_0 \ll a_{\text{cap}}$ imply that small disks will give way to larger rods as soon as end effects become sufficiently unimportant. The stability of finite disks against bilayer (lamellae) formation follows again from the fact that the rim is not too heavily disfavored compared to the cylindrical body. Tanford argues further that this is "probably a general result applicable to all systems in which relatively small micelles are formed, provided that one is dealing with reasonably dilute solutions." Indeed, his example of $\tilde{\mu}^0_{s,\text{disk}} - \tilde{\mu}^0_{s,\text{rod}}$ for SDS changes sign (for $s \gtrsim 250$) in much the way indicated in our Fig. 1, reinforcing again the idea (cf. Figs. 2A and B, also for $y \simeq 0.43$) that small disks yield at higher concentrations to larger rods. We have shown, however, that for greater interfacial tensions—and/or for smaller or larger y values—the disk-like micelles will be "squeezed out" by lamellae or rods.

[2] Tanford writes $\tilde{\mu}^0(a) = \gamma a + c/a + D/a^2 + E/a^3$, the last two terms comprising corrections to the Coulomb repulsion energy—but these empirically determined improvements are not of conceptual importance for our discussion. Similarly, he evaluates his surface areas not at a single l but rather at $l + \delta x$ where δx takes on different values according to whether the hydrophobic (γa) or repulsion ($c/a + \cdots$) contributions to $\tilde{\mu}^0$ are being considered; again, however, these details are not significant for present purposes except insofar as they affect the optimum head group area.

ACKNOWLEDGMENTS

We are happy to thank Dr. Andrew Masters, Dr. Jean Charvolin, and Dr. Yolande Hendrikx for helpful conversations on these researches. William M. Gelbart acknowledges financial support of this work by the National Science Foundation (Grant CHE80-24270), the Camille and Henry Dreyfus Foundation (Teacher-Scholar Award), and the Direction des Recherches Études et Techniques (Grant 82-1047). William E. McMullen thanks the Exxon Education Foundation for its financial assistance during this work, and Avinoam Ben-Shaul thanks similarly the Minerva Foundation.

REFERENCES

1. Ben-Naim, A., "Hydrophobic Interactions." Plenum, New York, 1980.

2. Tanford, C., "The Hydrophobic Effect," 2nd ed. Wiley, New York, 1980.
3. Israelachvili, J. N., Marcelja, S., and Horn, R. G., *Quart. Rev. Biophys.* **13,** 121 (1980).
4. Dill, K. A., and Flory, P. J., *Proc. Nat. Acad. Sci. USA* **77,** 3115 (1980) and **78,** 676 (1981).
5. Gruen, D. W. R., and de Lacey, E. H. B., "Proceedings of the International Symposium on Surfactants in Solution, held in Lund, Sweden, July 1982." Plenum, New York, in press.
6. Mukherjee, S., Miller, C. A., and Fort, T. Jr., *J. Colloid Interface Sci.* **91,** 223 (1983); Helfrich, W., *in* "Physique des Defauts: Les Houches" (R. Balian *et al.* Eds.), p. 716. North Holland, Amsterdam, 1980, and references cited therein.
7. Israelachvili, J. N., Mitchell, D. J., and Ninham, B. W., *J. Chem. Soc., Faraday Trans. II* **72,** 1525 (1976).
8. Hendrikx, Y., Charvolin, J., Rawiso, M., Liébert, L., and Holmes, M. C., *J. Phys. Chem.* **87,** 3991 (1983).
9. Yu, L. J., and Saupe, A., *Phys. Rev. Lett.* **45,** 1000 (1980).
10. Forrest, B. J., and Reeves, L. W., *Chem. Rev.* **81,** 1 (1981); and Amaral, L. W., Tavares, M. R., and Vanin, J. A., *J. Chem. Phys.* **71,** 2980 (1979).
11. Holmes, M. C., and Charvolin, J. C., *J. Phys. Chem.* (in press).
12. Jönsson, B., and Wennerström, H., *J. Colloid Interface Sci.* **80,** 482 (1981).
13. Gelbart, W. M., Ben-Shaul, A., and McMullen, W. E., *J. Phys. Chem.* (in press); and Ben-Shaul, A., and Gelbart, W. M., *J. Phys. Chem.* **86,** 316 (1982).
14. Wennerström, H., *J. Colloid Interface Sci.* **68,** 589 (1979).
15. Mazer, N. A., Benedek, G. B., and Carey, M. C., *J. Phys. Chem.* **80,** 1075 (1976).